Tauroursodeoxycholic Acid Preservation of Photoreceptor Structure and Function in the *rd10* Mouse through Postnatal Day 30

M. Joe Phillips,[1,2] *Tiffany A. Walker,*[1] *Hee-Young Choi,*[1,3] *Amanda E. Faulkner,*[1] *Moon K. Kim,*[1] *Sheree S. Sidney,*[2] *Amber P. Boyd,*[2] *John M. Nickerson,*[2] *Jeffrey H. Boatright,*[2] *and Machelle T. Pardue*[1,2]

Purpose. Retinitis pigmentosa (RP) is a progressive neurodegenerative disease resulting in blindness for which there is no current treatment. Although the members of the family of RP diseases differ in etiology, their outcomes are the same: apoptosis of rods and then by cones. Recently, the bile acid tauroursodeoxycholic acid (TUDCA) has been shown to have antiapoptotic properties in neurodegenerative diseases, including those of the retina. In this study the authors examined the efficacy of TUDCA on preserving rod and cone function and morphology at postnatal day 30 (P30) in the *rd10* mouse, a model of RP.

Methods. Wild-type C57BL/6J and *rd10* mice were systemically injected with TUDCA (500 mg/kg) every 3 days from P6 to P30 and were compared with vehicle (0.15 M $NaHCO_3$). At P30, retinal function was measured with electroretinography, and morphologic preservation of the rods and cones was assessed with immunohistochemistry.

Results. Dark-adapted electroretinographic (ERG) responses were twofold greater in *rd10* mice treated with TUDCA than with vehicle, likewise light-adapted responses were twofold larger in TUDCA-treated mice than in controls at the brightest ERG flash intensities. TUDCA-treated *rd10* retinas had fivefold more photoreceptors than vehicle-treated retinas. TUDCA treatments did not alter retinal function or morphology of wild-type mice when administered to age-matched mice.

Conclusions. TUDCA is efficacious and safe in preserving vision in the *rd10* mouse model of RP when treated between P6 and P30. At P30, a developmental stage at which nearly all rods are absent in the *rd10* mouse model of RP, TUDCA treatment preserved rod and cone function and greatly preserved overall photoreceptor numbers. (*Invest Ophthalmol Vis Sci.* 2008;49: 2148–2155) DOI:10.1167/iovs.07-1012

From the [1]Rehabilitation Research and Development Center, Atlanta VA Medical Center and the [2]Department of Ophthalmology, Emory School of Medicine, Atlanta, Georgia; and the [3]Department of Ophthalmology, Pusan National University, Pusan, Republic of Korea.

Supported by Department of Veterans Affairs, Foundation Fighting Blindness, Research to Prevent Blindness, Knights Templar Education Foundation, and the National Institutes of Health (Grants R01 EY014026, P30 EY06360, R01 EY012514, P30 AT000609, R24EY017045, and R01 EY016470).

Submitted for publication August 6, 2007; revised October 29 and December 19, 2007; accepted March 14, 2008.

Disclosure: **M.J. Phillips**, None; **T.A. Walker**, None; **H.-Y. Choi**, None; **A.E. Faulkner**, None; **M.K. Kim**, None; **S.S. Sidney**, None; **A.P. Boyd**, None; **J.M. Nickerson**, P; **J.H. Boatright**, P; **M.T. Pardue**, P

The publication costs of this article were defrayed in part by page charge payment. This article must therefore be marked "*advertisement*" in accordance with 18 U.S.C. §1734 solely to indicate this fact.

Corresponding author: Machelle T. Pardue, Rehabilitation Research and Development Center, Research Service (151 Oph), Atlanta VA Medical Center, 1670 Clairmont Road, Decatur, GA 30033; mpardue@emory.edu.

Retinitis pigmentosa (RP) is a family of diseases characterized by night blindness and loss of peripheral vision followed by progressive loss of central vision. RP affects approximately 50,000 to 100,000 people in the United States and approximately 1.5 million people worldwide.[1] Currently, approximately 200 genes have been identified that cause RP or related retinal diseases (http://www.sph.uth.tmc.edu/Retnet/), showing the genetic diversity of this group of diseases. However, regardless of the mutation, the final common pathway is programmed photoreceptor cell death, or apoptosis.[2]

Bear bile has a history of positive effects in ancient Chinese medicine,[3,4] but Western medicine has only recently investigated the antiapoptotic effects of bile acids, including tauroursodeoxycholic acid (TUDCA), the taurine conjugate of ursodeoxycholic acid (UDCA). The bulk of the therapeutic effects of TUDCA and UDCA have been shown in the treatment of a wide range of liver and gall bladder diseases.[5–7] More recently, TUDCA has been shown to be neuroprotective in animal models of Huntington disease,[8,9] Parkinson disease,[10] and acute stroke.[11,12] TUDCA and UDCA are antiapoptotic agents, and though the exact mechanisms of apoptosis prevention are still under investigation, several key signaling pathways have been implicated. TUDCA modulates cell cycle effector genes, including cyclin D1 and P53.[13–17] Phosphytidal-inositol-3-kinase,[18–20] mitogen-activated protein kinase,[20] and ERK/Akt[21] pathway activation have all been implicated in TUDCA administration. TUDCA and UDCA also stabilize the mitochondrial membrane. They directly inhibit mitochondrial permeability transition, inhibit cytosolic Bax translocation, and suppress mitochondrial release of cytochrome *c*.[22,23] Bile acids block reactive oxygen intermediate production[22–24] and may themselves be antioxidants.[23] They block caspase activation, including caspase-3[12,22,23,25] and also prevent inactivation of the nuclear enzyme poly(ADP-ribose)polymerase.[12,22,23]

Because of the prominent role of apoptosis in retinal degenerative disease, TUDCA was tested in the *Pde6b*^{rd10} (*rd10*) mouse. The *rd10* mouse has a missense point mutation in exon 13 of the β-subunit of the rod cGMP phosphodiesterase (β-PDE).[25–27] Thus, the *rd10* mouse is similar to the popular *Pde6b*^{rd1} or *rd1* mouse, which also shares a mutation in β-PDE gene.[28,29] The rate of degeneration in the *rd10* mice is similar to that in the *rd1* mutant model with a delayed onset; both have rapid rod degeneration followed by cone degeneration.[25–27,30]

In a previous study, TUDCA treatment of *rd10* mice showed significant preservation of photoreceptor function and morphology at postnatal day (P) 18.[25] In the *rd10* mice, maximal retinal cell loss on a C57BL/6J background occurs at approximately P28.[30] Rods degenerate faster than cones in *rd10* mice, with rod function decreased by approximately 70% under dark-adapted conditions, whereas cone-isolating, light-adapted conditions show a 50% decline at P30.[26] Furthermore, though rod degeneration appears nearly complete by P40 in *rd10* mice,[26] cones have been identified until 9 months of age.[30]

Investigative Ophthalmology & Visual Science, May 2008, Vol. 49, No. 5

The present study tests the hypothesis that TUDCA preserves rods and cones to P30, the stage at which photoreceptor cell loss peaks.[30] At this stage of degeneration in the *rd10* model, most rods have degenerated, and only some cones remain.[26] This stage of degeneration represents the end stage of RP for most patients because it is estimated that only 0.5% of RP patients develop complete blindness (no light perception).[31] Thus, these experiments test the efficacy of TUDCA at a critical stage of degeneration. To test this hypothesis, *rd10* mice were treated with TUDCA or vehicle from P6 to P30, and rod and cone function and morphology were assessed by electroretinography, histology, immunohistochemistry, and TUNEL labeling. Although TUDCA and UDCA have been shown to be very well tolerated in animals[8–12] and humans[32] (UDCA has received US Food and Drug Administration approval), these studies have all been performed in adult animals. Thus, in this study, we also sought to determine whether the antiapoptotic affects of TUDCA had an effect on early retinal development by treating age-matched C57BL/6J wild-type (WT) mice at the same time points. These studies demonstrate that TUDCA is effective in preserving photoreceptors in the *rd10* mice at P30.

Materials and Methods

Animals

All animal procedures were approved by the Institutional Animal Care and Use Committee at the Atlanta VA Medical Center and conform to the standards of the ARVO Statement for the Use of Animals in Ophthalmic and Vision Research. To establish a breeding colony, *Pde6b*^{rd10} mice on a C57BL/6J background (or *rd10*) were obtained from Jackson Laboratories (Bar Harbor, ME). All mice were housed under controlled lighting conditions on a 14-hour light/10-hour dark cycle (25–200 lux). Each litter was randomly divided at P6 to receive TUDCA treatment (500 mg/kg; Calbiochem, San Diego, CA; $n = 17$) or vehicle (0.15 M $NaHCO_3$, 1 mL/kg, pH 7.0; Sigma, St. Louis, MO; $n = 14$). A breeding colony of WT C57BL/6J mice (Jackson Laboratories, Bar Harbor, ME) received the same treatments as the *rd10* mice ($n = 5$ for TUDCA, $n = 2$ for vehicle treatment) starting at P6. TUDCA and vehicle solutions were made up fresh before every injection and were pH adjusted to 7.4.[25] Mice were weighed and injected once every 3 days beginning at P6 and ending at P30, resulting in eight total administrations per animal for the treated and vehicle groups. All injections were made subcutaneously at the nape of the neck.

Electroretinographic Methods

Mice were dark adapted overnight, and electroretinography was performed at P30 with a commercial recording system (UTAS 3000; LKC Technologies, Gaithersburg, MD).[25,33,34] After anesthesia induction (ketamine, 80 mg/kg; xylazine, 16 mg/kg), the cornea was anesthetized (1% tetracaine), and the pupils were dilated (1% tropicamide, 1% cyclopentolate). Body temperature was maintained at 37°C by placing the mice on a heating pad inside a Faraday cage. The active electrode consisted of a silver wire loop that was positioned on the cornea using 1% methylcellulose. Needle electrodes placed in the cheek and tail served as reference and ground, respectively. A desktop Ganzfeld was used to administer a series of increasingly intense light flashes ranging from −3.0 to 2.1 log cd · s/m^2. Dark-adapted ERG recordings were averaged over 5 to 10 separate flashes per light intensity, with the interstimulus time increasing from 10 to 60 seconds as the flash intensity increased. Animals were then light adapted for 10 minutes using a steady background light (30 cd/m^2). Cone-isolating responses were recorded to a seven-step intensity series (−0.82 to 1.88 log cd · s/m^2) presented at 3 Hz in the presence of the same light-adapting background. Light-adapted ERGs were averaged over 25 separate flashes per intensity.

ERG a-wave amplitudes were measured from baseline to the first negative wave. The b-wave was measured from the trough of the a-wave to the peak of the first positive wave or, when the a-wave was not present, from baseline to the peak of the first positive wave. Implicit time measurements were made from flash onset to the trough or peak of the a- or b-wave, respectively. Statistical analysis across flash intensity and between treatment groups was conducted by using repeated measures ANOVA tests (SPSS, Chicago, IL).[25,33]

Histologic Methods

After ERG recordings, deeply anesthetized mice were killed by cervical dislocation. Eyes were immediately enucleated. Fixative was injected into the superior limbus to mark orientation and to aid in the rapid fixation of the retina. All left eyes were immersion fixed in 4% paraformaldehyde for 30 minutes for TUNEL labeling, and all right eyes were fixed overnight in 2.5% glutaraldehyde/2% paraformaldehyde for light microscopy. After fixation, right eyes were dehydrated through a graded alcohol series, infiltrated with propylene oxide, and embedded in resin (Epon 812/Der 736; Electron Microscopy Sciences, Hatfield, PA). Sections (0.5 μm) bisecting the optic disc superiorly to inferiorly were then cut on an ultramicrotome (UltraCut; Leica, Chicago) using a histodiamond knife and collected on glass slides. Slides were stained with 1% aqueous toluidine blue (Sigma, St. Louis, MO).

Left eyes were processed through a graded series of alcohols and embedded in paraffin. Sections (5-μm thick) were cut on a rotary microtome, bisecting the optic disc superiorly to inferiorly. Paraffin sections were used for cone opsin immunolabeling and TUNEL stain.

Total Photoreceptor Cell Counts

Plastic sections were analyzed using light microscopy (DMRB; Leica, Bannockburn, IL) to determine photoreceptor cell counts. Four retinal regions in the vertical meridian (0.5 mm in width) were photographed at 20× magnification. Locations in reference to the optic nerve head were 2.0 to 1.5 mm superior, 1.0 to 0.5 mm superior, 0.5 to 1.0 mm inferior, and 1.5 to 2.0 mm inferior. Photoreceptor nuclei counts were performed using image software (Plus 5.0; ImagePro, Silver Spring, MD). Three sections were counted for each of the four retinal areas in each eye. These values were then averaged, and analysis of variance (ANOVA; SPSS 8.0; SPSS, Inc., Chicago, IL) was performed.

Cone Photoreceptor Labeling

Paraffin sections were deparaffinized with xylene, followed by a graded series of alcohol rinses. After an initial blocking step with 5% goat serum (Chemicon, Temecula, CA) made with blocking buffer (Superblock; Pierce, Rockford, IL), sections were incubated in antiopsin green/red and blue (1:500; Chemicon) for 48 hours at room temperature. The primary antibody was visualized by labeling with goat anti-rabbit IgG secondary antibody (1:500; Alexa-Fluor 488; Abcam, Cambridge, MA) for 1 hour, after optimization with a titrated series for both the primary and the secondary antibody. Each slide contained a negative control by eliminating primary antibody from one section per slide. Sections were then coverslipped with an aqueous mounting medium (Gel/Mount; Biomeda, Foster City, CA). Digital micrographs were captured of images at 20× magnification using a confocal microscope. All micrographs were taken from sections stained the same day with the same camera settings.

Cone Photoreceptor Nuclei Counts

Rod and cone photoreceptor nuclei have differently shaped heterochromatin such that rods have a dense central clump and cones have irregularly shaped heterochromatin that can appear as one to three clumps in tissue sections.[35,36] Thus, cone photoreceptor nuclei were quantified by counting all photoreceptor nuclei with two or more clumps of heterochromatin[35] in toluidine blue–stained plastic sections (see Fig. 5 for examples of cone vs. rod photoreceptor nuclei). Using the same plastic sections and retina regions described, three indepen-

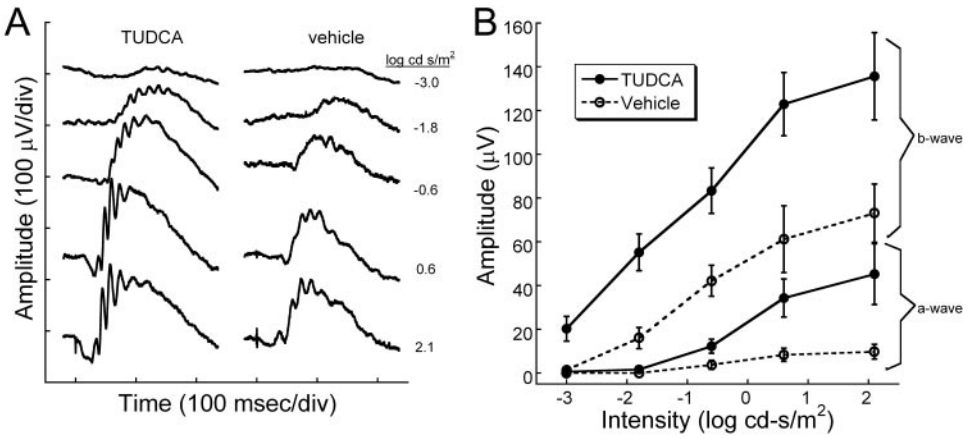

FIGURE 1. Dark-adapted retinal function in *rd10* mice after TUDCA treatment at P30. ERG recordings showing rod-dominated retinal function in P30 *rd10* mice treated with TUDCA or vehicle. (**A**) Representative ERG waves to a series of flash intensities from a TUDCA- or vehicle-treated mouse. At every light level, the TUDCA-treated mice had a larger response than the vehicle-treated *rd10* mouse. The a-wave is much larger in the TUDCA-treated animals. (**B**) Plot of average ERG amplitude (±SEM) for a- and b-waves from the two treatment groups. TUDCA ($n = 16$) and vehicle ($n = 10$). TUDCA-treated animals had significantly greater a- and b-wave amplitudes than the vehicle groups (repeated-measures ANOVA; a-wave, $F(4, 88) = 2.66$, $P = 0.038$; b-wave, $F(4, 96) = 2.55$ $P = 0$). We conclude that TUDCA is efficacious in preventing the loss of ERG signals in response to a range of scotopic flashes.

dent observers counted cone nuclei at 20×. Different treatment groups and strains were compared using ANOVA (SPSS 8.0; SPSS).

TUNEL Labeling

Paraffin sections were stained by terminal deoxynucleotidyl transferase-mediated 2′deoxyuridine 5′triphosphate-biotin nick end labeling (TUNEL) using a TUNEL kit (DeadEnd Fluorometric; Promega, Madison, WI) according to the manufacturer's kit instructions and were counterstained with propidium iodide.[25] Images of TUNEL-stained sections were captured by computer-aided confocal microscopy, and photoreceptor nuclei were counted per field at 20× magnification as described. For each field, ANOVA was used to compare the means between the treatment groups (SPSS 8.0; SPSS).

RESULTS

Results are broken into two broad sets of experiments, those dealing with the efficacy of TUDCA in the *rd10* mouse model of RP and those testing TUDCA in age-matched WT mice with the same doses.

Efficacy of TUDCA in the *rd10* Mouse

TUDCA Preserves Retinal Function at P30. To determine whether TUDCA treatments preserved rod and cone function in *rd10* mice, we performed dark- and light-adapted electroretinography at P30. We found that TUDCA treatment significantly preserved both rod and cone function in *rd10* mice. Comparing TUDCA- and vehicle-treated mice, dark-adapted ERGs from TUDCA-treated animals showed significantly larger waveforms (Fig. 1A). At the highest flash intensity, the a-wave amplitude was approximately five times larger in TUDCA-treated mice than in the control treatment groups, whereas the b-wave amplitude was twice as large as were the other treatment groups (Fig. 1). Furthermore, mice treated with TUDCA showed significant preservation of mean a- and b-wave amplitudes (Fig. 1B) over a range of ERG flash intensities, as assessed by repeated-measures ANOVA (a-wave: $F(4, 88) = 2.66$, $P = 0.038$; b-wave: $F(4, 96) = 2.55$, $P = 0.044$; $n = 16$ for TUDCA-treated group; $n = 10$ for vehicle-treated group).

Cone-mediated, light-adapted ERG waveforms were significantly larger in TUDCA-treated *rd10* mice than in vehicle (Fig. 2A). In the representative waveforms shown in Figure 2A, the electroretinogram from the TUDCA-treated animal was clearly larger in amplitude at all intensities, and the b-wave threshold was measurable at -0.8 log cd · s/m^2 compared with -0.4 log cd · s/m^2 for the vehicle-treated animal. When amplitude was plotted across flash intensity, it was seen that there are significant differences in b-wave amplitude between the treatment groups at the brightest flashes ($n = 15$ TUDCA; $n = 10$ vehicle; repeated-measures ANOVA $F(6, 138) = 6.364$; $P < 0.001$). No

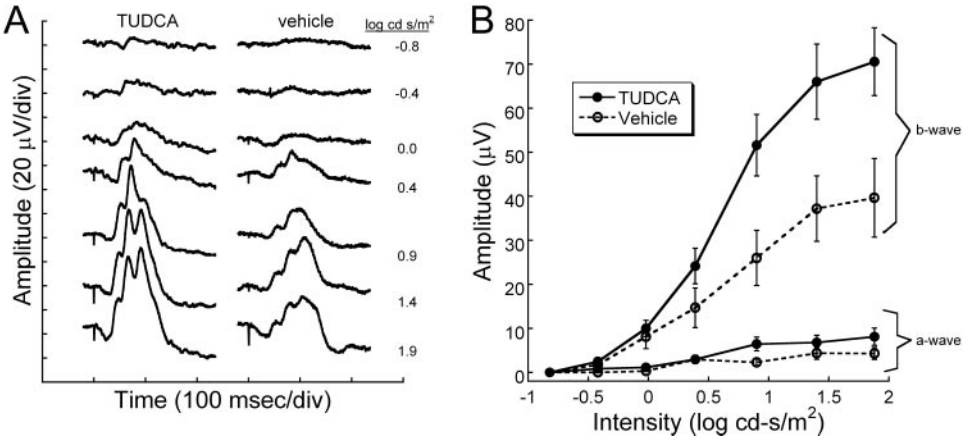

FIGURE 2. Light-adapted retinal function after TUDCA treatment in *rd10* mice at P30. (**A**) ERG waves recorded in response to a series of Ganzfeld flashes in the presence of an adapting background light (30 cd/m^2). The vehicle-treated mouse shows a slight decrease in sensitivity with the first recordable response at -0.4 log cd · s/m^2. At the brightest flashes, the TUDCA-treated mouse had ERG b-wave amplitudes that were twice the size of those of the vehicle-treated control. (**B**) Average ERG amplitudes (± SEM) for light-adapted a- and b-waves are plotted across intensity. The cone-mediated b-wave in the TUDCA-treated group ($n = 15$) is significantly different than in the vehicle group ($n = 10$) ($F(6,138) = 6.364$, $P < 0.001$). The a-wave amplitude is not statistically significantly different between the groups (repeated-measures ANOVA; $F(6, 120) = 2.075$, $P = 0.061$). We conclude that TUDCA is efficacious in preserving cone-mediated electrical responses in the retina.

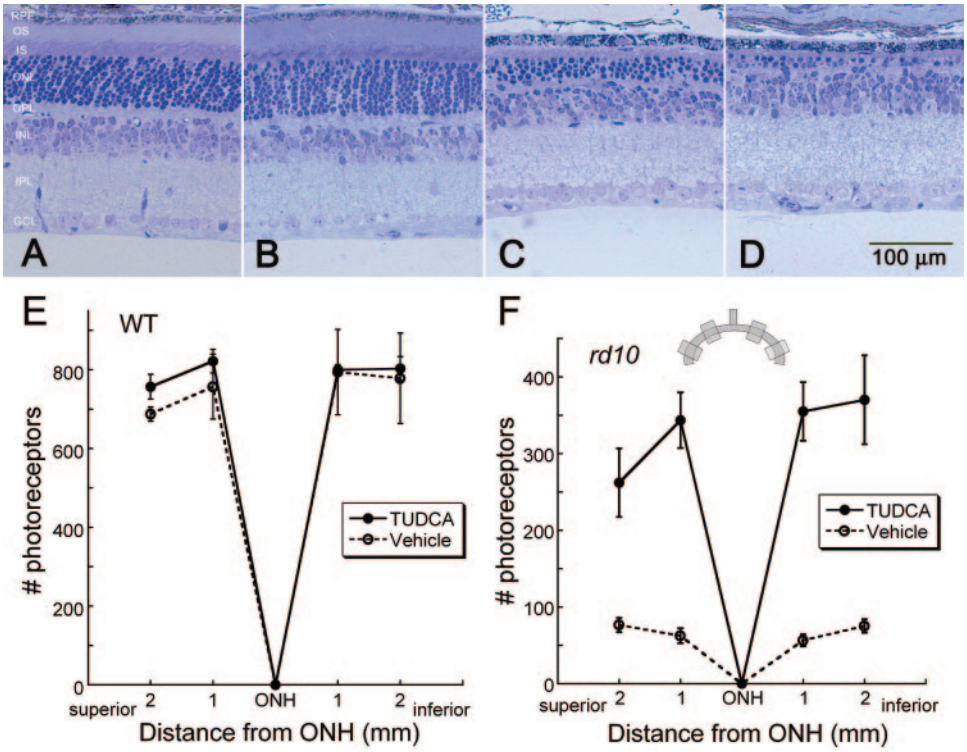

FIGURE 3. Retinal morphology after TUDCA treatment at P30. Retinal micrographs from P30 WT C57BL/6 mice treated with TUDCA (**A**) or vehicle (**B**). All retinal layers are intact, and the photoreceptor layers are normal. Qualitatively, (**A**) and (**B**) show no changes between treatment groups in any of the layers of the retina of WT mice. This finding suggests that TUDCA treatment at the given dose and for the indicated duration is safe. Retinal micrographs from *rd10* mice treated with TUDCA (**C**) or vehicle (**D**). The photoreceptor layer has been reduced to approximately 1 row of nuclei in the vehicle-treated mouse (**D**), whereas the TUDCA-treated retina retains three to four rows of nuclei (**C**). (**C**) and (**D**) show clear differences in the thicknesses of the ONL, outer segments (OS), and inner segments (IS), with TUDCA treatment demonstrating an efficacious delay of retinal degeneration. (**E**, **F**) Plots of the total number of photoreceptors at each retinal location from WT and *rd10* mice with reference to the optic nerve. *Inset*: schematic diagram of the retina and optic nerve. Each *shaded square* indicates a sampling region, as indicated on the graphs. (**E**). Photoreceptor cell counts in the WT mice from the two treatment groups show no differences across the retina. (n = 5 TUDCA, n = 2 vehicle, ANOVA $F(3, 12) = 0.397$, $P = 0.757$) (**F**). Photoreceptor cell counts from *rd10* mice treated with TUDCA (n = 17) or vehicle (n = 14). The TUDCA-treated mice have significantly more photoreceptors across all areas sampled than vehicle-treated mice (ANOVA $F(3, 87) = 3.013$, $P = 0.034$). We conclude that TUDCA treatment is efficacious in preventing or slowing photoreceptor degeneration up to P30 in the *rd10* mouse model of RP.

significant differences were detected between the treatment groups for the small light-adapted a-wave (repeated-measures ANOVA $F(6, 120) = 2.075$; $P = 0.061$).

Preservation of Photoreceptor Nuclei: Rod and Cone Photoreceptors. To determine whether TUDCA treatments preserved photoreceptors, we examined photoreceptor structure and numbers in *rd10* mice. TUDCA treatments significantly preserved photoreceptor numbers and the inner and outer segments in the *rd10* mice (Fig. 3C) compared with vehicle-treated controls (Fig. 3D). The number of photoreceptor nuclei in a 0.5-mm field at four locations from inferior to superior in TUDCA-treated *rd10* mice at P30 showed significant preservation of photoreceptors (Fig. 3F; ANOVA $F(3, 87) = 3.013$; $P < 0.034$). TUDCA-treated *rd10* retinas contained an average of 333 ± 44 photoreceptor nuclei per region compared with only 68 ± 9 photoreceptor nuclei per 0.5-mm region in the vehicle-treated *rd10* retina (mean ± SEM; Figs. 3C, 3D, 3F), a fivefold preservation.

Preservation of Photoreceptor Nuclei: Cone Photoreceptors. To identify the population of cone photoreceptors, paraffin sections were labeled with anticone opsin. Immunolabeled WT retinas showed distinct labeling of cone photoreceptor outer segments (Fig. 4A), as previously reported.[37,38] The labeled cone outer segment of WT mice always appeared long and had a distinct tip (Fig. 4A). In TUDCA-treated *rd10* retinas, distinct cone labeling was still visible (Figs. 4B, 4C). Labeled segments correlated with the extent of preservation. Retinas with the most preservation of photoreceptors and longer outer segments had the most cone labeling (Fig. 4B). In *rd10* mice with less preservation from the TUDCA treatments, the cone outer segments were smaller and the cone opsin labeling appeared as small round structures or punctuate in the region of the outer segments (Fig. 4C). In vehicle-treated *rd10* mice, the outer segments were not visible, and cone opsin labeling was seen as only small punctuate labeling (Figs. 4D, 4E). Although some variability in cone opsin labeling was present in all treatment groups, TUDCA-treated retinas more frequently presented with a continuous line of outer segments and longer cone outer segments compared with vehicle-treated retinas (Figs. 4B, 4C vs. 4D, 4E).

Cone nuclei were quantified by counting in toluidine blue plastic-embedded sections. All photoreceptor nuclei with two or more clumps of heterochromatin were classified as cones.[35] Figure 5A (arrows) shows cone nuclei in a WT retina, whereas Figure 5B (arrows) shows cone nuclei identified in an *rd10* TUDCA-treated retina. Figure 5C shows that average cone nuclei counts across the retinal areas from TUDCA- and vehicle-treated *rd10* retinas were similar, 2.92 ± 0.27 versus 4.08 ± 0.49 cones/500 μm (TUDCA, n = 14; vehicle, n = 11; ANOVA $F(3, 69) = 1.25$, $P = 0.298$). In addition, no differences in cone counts in WT retinas were found between treatment groups (Student's t-test, $P = 0.93$). WT mice had 10.5 ± 1.1 nuclei/500 μm (significantly more cone nuclei than *rd10* mice), as expected (Student's t-test, $P < 0.001$).

Apoptosis in the *rd10* Retina at P30

We have previously shown that *rd10* retinas at P18 have numerous TUNEL-positive nuclei, but TUDCA-treated retinas have few apoptotic nuclei.[25,26] Thus, at P30, we expect to see fewer TUNEL-positive nuclei in vehicle-treated retinas because of the prior massive loss of photoreceptors before this stage. In contrast, because of the delay in degeneration produced by TUDCA treatments, we expect to observe some apoptotic nuclei in TUDCA-treated retinas.

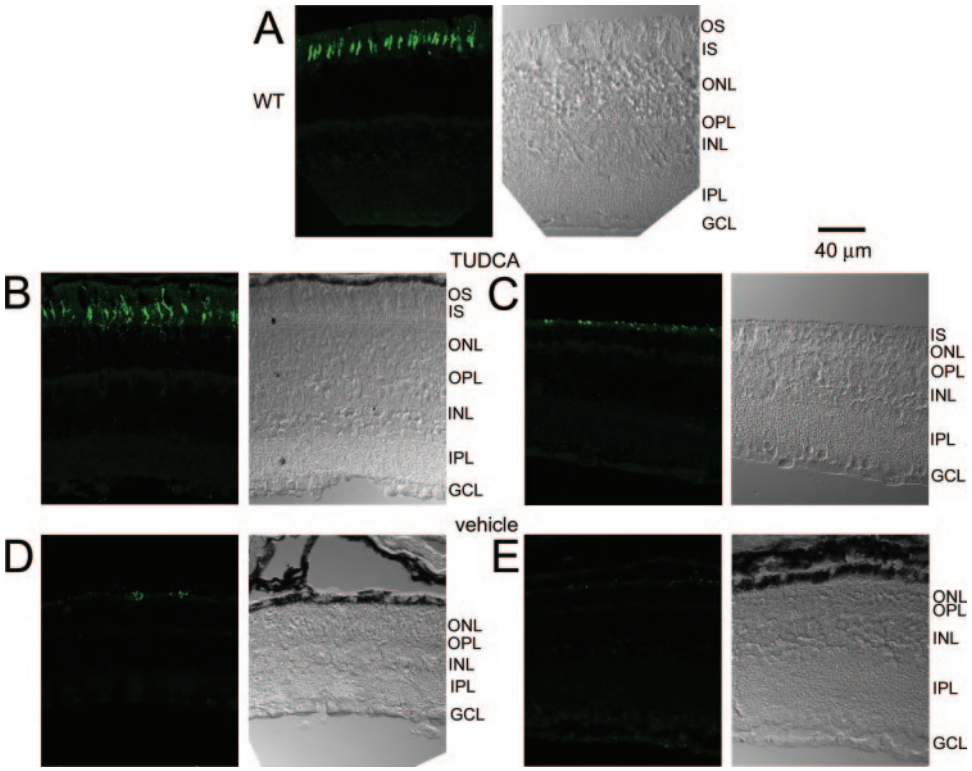

FIGURE 4. Cone opsin labeling in WT and *rd10* mice after TUDCA treatments at P30. Each micrograph is presented as a pair, with the DIC image on the *right* and the cone opsin labeling on the *left*. (**A**) Cone opsin immunohistochemistry in a WT retina showing distinct outer segments of cones. (**B**, **C**) TUDCA-treated *rd10* retinas showing long cone outer segments, similar to WT retina (**B**) and shorter cone outer segments with more punctuate labeling (**C**). (**D**, **E**) Cone labeling in vehicle-treated *rd10* retinas appeared as sparse punctuate labeling. Note that no outer segments are visible in the DIC images of the vehicle-treated mice. These results suggest that TUDCA treatments preserve cone outer segments.

Our results show that TUDCA-treated *rd10* retinas and vehicle-treated retinas had similar numbers of apoptotic nuclei. The average number of TUNEL-positive nuclei in TUDCA-treated retinas per microscope field was 6.8 ± 1.1 (mean ± SEM; $n = 10$) compared with 11.2 ± 2.9 ($n = 3$) in vehicle-treated retinas. These differences were not significant (Student's *t*-test, $P = 0.29$).

TUDCA Studies in WT Mice

TUDCA Treatment Does Not Affect Normal Retinal Function. To test whether TUDCA has adverse affects on normal retinal function when given early in development, we recorded electroreginograms from TUDCA- and vehicle-treated mice. Figure 6A shows the typical dark-adapted ERG waveform to a series of flash intensities. Waveforms from TUDCA-treated retinas were larger than those from vehicle-treated retinas. The mean dark-adapted ERG amplitudes for the a- and b-waves were nearly identical for the TUDCA- and vehicle-treated mice (Figs. 6B, 6C; repeated-measures ANOVA, $F(4, 20) = 2.020$, $P = 0.130$, and $F(4, 20) = 3.110$, $P = 0.138$, respectively; $n = 5$ for TUDCA-treated and $n = 2$ for vehicle-treated). Light-adapted b-wave amplitudes were also similar between treatment groups (Fig. 6D; repeated-measures ANOVA, $F(6, 30) = 0.532$, $P = 0.779$).

TUDCA Treatment Does Not Affect Normal Retinal Morphology. Retinal morphology appeared normal in WT mice from all treatment groups (Figs. 3A, 3B, 3E). The average number of photoreceptor nuclei was similar, with 795.4 ± 27.4 and 754.2 ± 46.9 nuclei/region in TUDCA-treated and vehicle-treated retinas, respectively. The number of nuclei

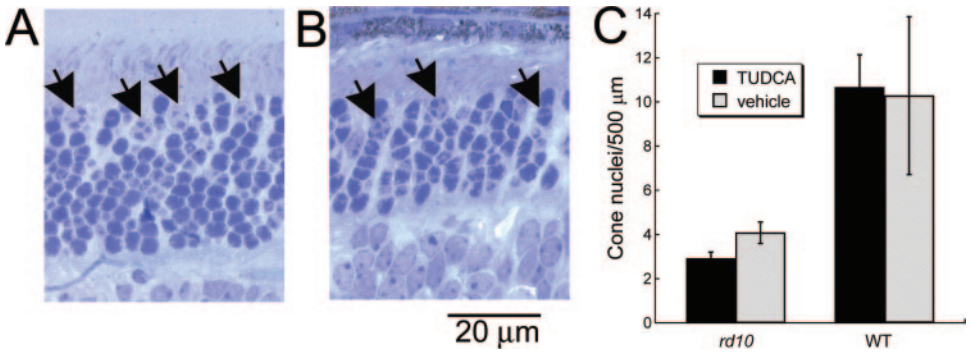

FIGURE 5. Quantitative assessment of cones after TUDCA treatment at P30. Cone nuclei in WT (**A**) and *rd10* (**B**) mice were counted based on heterochromatin pattern. Heterochromatin that formed two or more clumps was counted as a cone (*arrows*) according to the criteria established by Carter-Dawson and LaVail.[35] This contrasts with rod nuclear staining, which appears dark and uniformly stained. (**C**) Cone counts for each 500-μm retinal region did not show any differences between treatment groups for *rd10* or WT mice. However, WT mice had two to three times more cone nuclei per retinal area than *rd10* mice (Student's *t*-test, $P < 0.001$). Error bars indicate SEM.

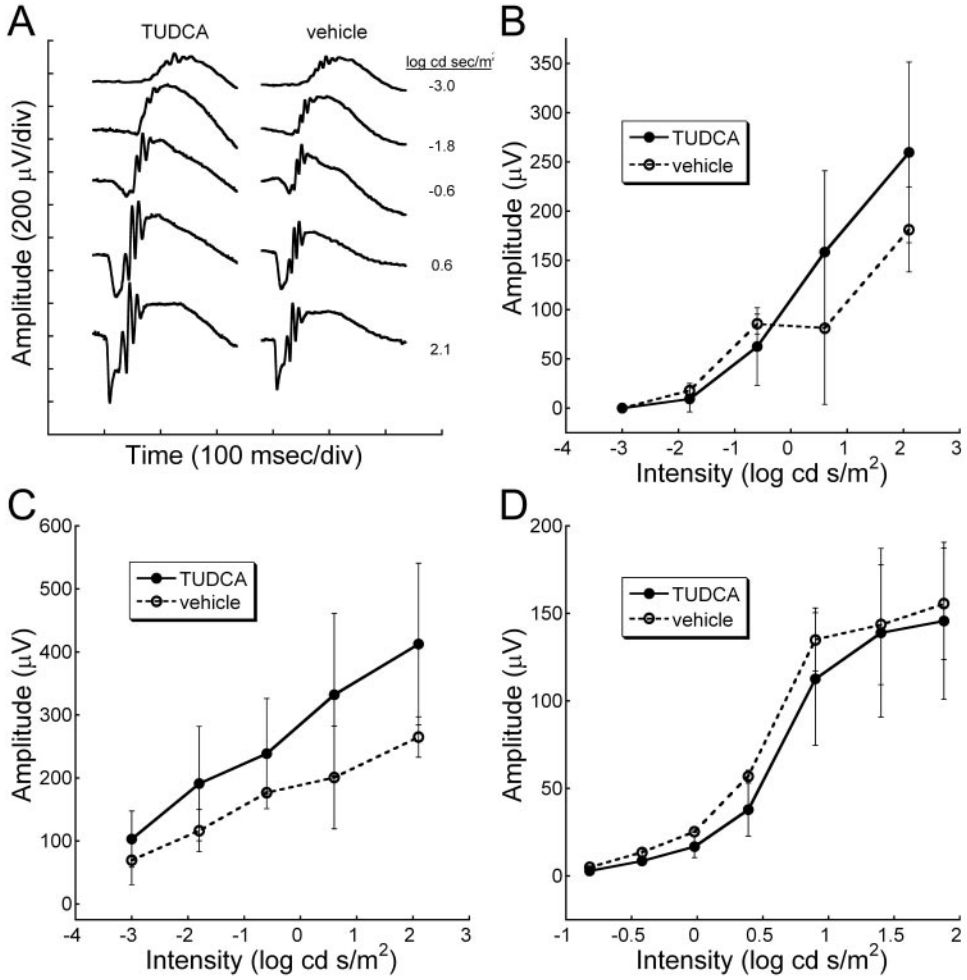

FIGURE 6. Studies in WT mice. Retinal function measurements were recorded from WT C57BL/6J mice treated with TUDCA or vehicle from P6 to P30. (**A**) Representative dark-adapted ERG waveforms for WT TUDCA- and vehicle-treated mice. Dark-adapted a-wave (**B**), dark-adapted b-wave (**C**), or light-adapted b-wave (**D**) amplitudes from WT mice treated with TUDCA ($n = 5$) or vehicle ($n = 2$) show no differences in amplitude or timing across different flash intensities (repeated-measures ANOVA $F(4, 20) = 2.020$, $P = 0.130$; $F(4, 20) = 3.110$, $P = 0.138$; $F(6, 30) = 0.532$, $P = 0.779$; respectively). We concluded that TUDCA treatment from P6 to P30 has no deleterious effect on retinal function, as measured with the ERG.

across retinal areas was not significant between treatment groups in the WT mice (repeated-measures ANOVA, $F(3, 12) = 0.397$, $P = 0.757$; Fig. 3E).

TUDCA Treatment Alters Body Weight in *rd10* and WT Mice. Animal weights were also compared across time with TUDCA versus vehicle treatment. TUDCA-treated WT mice were found to have significantly lower body weights than vehicle-injected mice (Fig. 7A; repeated-measures ANOVA, $F(5, 25) = 4.276$, $P = 0.006$). As treatments progressed, the TUDCA-treated mice gained less weight than did vehicle-treated mice. The largest differences were not reached until P24. TUDCA-treated *rd10* mice also showed a significant decrease in body weight over the treatment period (Fig. 7B; repeated-measures ANOVA, $F(7, 245) = 10.973$, $P < 0.001$). In *rd10* mice, the effect of TUDCA on body weight was apparent by P9, much sooner than in the WT mice.

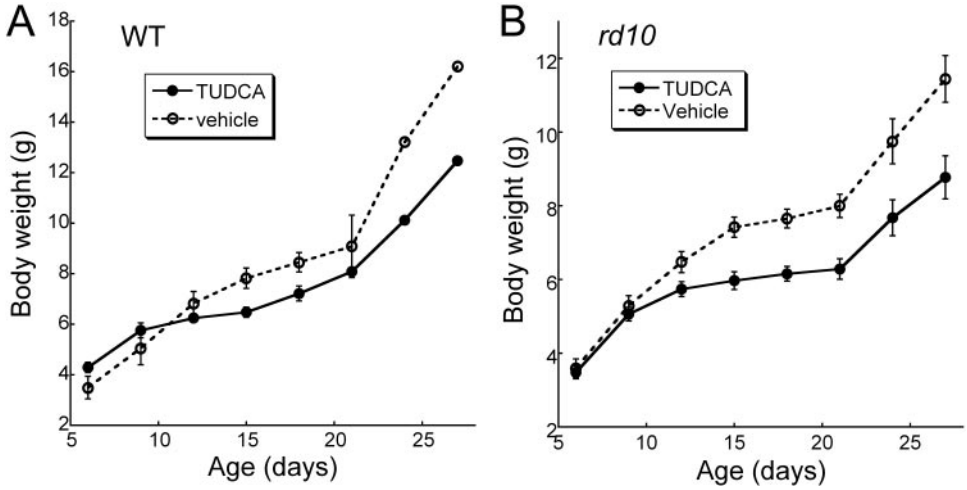

FIGURE 7. Body weights in WT and *rd10* mice after TUDCA treatments from P6 to P30. (**A**) WT mice treated with TUDCA ($n = 5$) showed a reduction in body weight compared with vehicle ($n = 2$; repeated-measures ANOVA $F(5, 25) = 4.276$, $P = 0.006$). (**B**) TUDCA-treatment of *rd10* mice ($n = 24$) resulted in significantly lower body weight than vehicle ($n = 13$) from P15 to P27 (repeated-measures ANOVA $F(7, 245) = 10.973$, $P < 0.001$). We conclude that TUDCA treatments suppressed body weight in the WT and *rd10* mice. Symbols represent mean ± SD.

Discussion

The present study demonstrates that TUDCA treatment, through the advanced degenerative time point of P30 in the *rd10* mouse, is remarkably effective in sustaining photoreceptor cells and their function. We have previously shown successful preservation of rod function and structure through P18 in this model.[25] Though slightly delayed compared with that in *rd1* mice, retinal degeneration in *rd10* mice is rapid and aggressive. In untreated *rd10* mice, the outer nuclear layer (ONL) is reduced to a single nuclear layer by P30.[25–27] Functionally, the dark-adapted a-wave is largely undetectable (only 3% of WT response), and the b-wave is greatly diminished (14% of WT response).[25–27] At this stage, rods are almost completely absent and cones are degenerating. This study shows that TUDCA treatments starting at P6 sustain retinal function and morphology through this critical stage from 30% (dark-adapted a-wave) to 45% (light-adapted and dark-adapted b-waves and photoreceptor numbers) of WT responses. These results show significant preservation of the retina by a systemic agent at this stage of degeneration.

A pan-retinal preservation of retinal function and photoreceptor nuclei was found in the TUDCA-treated *rd10* mice at P30. Rod function and rod photoreceptors were significantly greater in TUDCA-treated *rd10* mice (Figs. 1–3). In addition, the number of total photoreceptor nuclei was fivefold greater in TUDCA-treated mice than in vehicle-treated mice (Fig. 3).

Interestingly, TUDCA treatments appeared to preserve cone outer segment morphology compared with vehicle treatment (Fig. 4), which correlates well with the increased amplitudes in the light-adapted TUDCA-treated retinas (Fig. 2). However, no differences were found in the number of cone nuclei between the treatment groups (Fig. 5). These data may suggest that TUDCA causes an overall increase in preservation of the photoreceptors. Given that cone degeneration occurs secondarily in this model, the significant preservation of rods from TUDCA treatments may sustain the cones. A later time point may be needed to exclusively evaluate the effect of TUDCA treatments on cone preservation. However, because humans rely most on cone vision, the finding of greater cone function and healthier cone outer segments after TUDCA treatments suggests that this drug might be useful for preserving cone vision in people.

The similarity in TUNEL labeling between TUDCA- and vehicle-treated *rd10* retinas may suggest that TUDCA is delaying the death of photoreceptors in the *rd10* model. In our analysis of *rd10* retinas at P18, vehicle-treated retinas showed a vastly greater number of TUNEL-positive nuclei compared with TUDCA-treated retinas.[25] At P30, as might be expected, the vehicle-treated *rd10* retinas do not have many nuclei remaining to undergo apoptosis. Conversely, the TUDCA-treated retinas have many remaining nuclei, some of which are apoptotic. WT mice showed no significant differences between the treatment groups.

Similar to other studies that showed TUDCA to be well tolerated in adult animals,[8–12] we found no evidence at the functional or morphologic level that TUDCA itself had any significant adverse effects on the retina in WT mice when given from P6 to P30. However, TUDCA treatments did produce a decrease in body weight in WT and *rd10* mice (Fig. 7). The mean body weight of TUDCA-treated WT mice dropped 22%, whereas weights in TUDCA-treated *rd10* mice decreased 23%. These values are slightly below the 25% loss of body weight that is considered an end point criterion by our Institutional Animal Care and Use Committee. Other studies have not reported a reduction in body weight after TUDCA treatment, perhaps because other animal models were treated during adulthood[8–12] and not early postnatal development, as in this study. Future studies will determine whether a different vehicle would have less effect on body weight. Nevertheless, the lack of toxic effects on the retina complement other studies that showed the safety of UDCA treatment in human patients with liver disease,[32,39] of TUDCA treatment in rodent models of Huntington disease,[8,9] and of TUDCA treatment in rodent models of stroke.[11,12] If TUDCA continues to show effects on body weight in young animals, drug delivery approaches could be pursued to administer TUDCA exclusively to the retina.

Comparing the preservation of the *rd10* retina between P18 and P30, TUDCA appears to delay degeneration in *rd10* mice by approximately 12 days, or approximately 35%, over the course of the degeneration period. Because it has been reported that different species have surprisingly similar rates of degeneration based on maximal life expectancy[40] and that typical RP patients have a linear rate of retinal function loss,[41] a prediction of TUDCA ability to preserve vision in RP patients can be made. TUDCA might preserve retinal function for approximately 18 years in a patient whose photoreceptor loss began in his or her 20s and ended in his or her 70s. Coupling this possibility of efficacy with the demonstrated lack of toxicity of hydrophilic bile acids in several animal models[8–12] and humans[32,39] suggests that hydrophilic bile acids may be relevant to the ophthalmic clinic.

References

1. Berson EL. Retinitis pigmentosa: unfolding its mystery. *Proc Natl Acad Sci U S A*. 1996;93:4526–4528.
2. Reme CE, Grimm C, Hafezi F, Marti A, Wenzel A. Apoptotic cell death in retinal degenerations. *Prog Retin Eye Res*. 1998;17:443–464.
3. Cidian ZYD. *Dictionary of Traditional Chinese Medicine*. Shanghai: Shanghai Sci and Technology Press; 2004.
4. Williamson DF, Phipps MJ. *Proceedings in the Third Annual Symposium on the Trade in Bear Parts 1999*. Hong Kong: TRAFFIC East Asia; 2001.
5. Hofmann AF. Medical treatment of cholesterol gallstones by bile desaturating agents. *Hepatology*. 1984;4(suppl):199S–208S.
6. Crosignani A, Battezzati PM, Setchell KD, et al. Tauroursodeoxycholic acid for treatment of primary biliary cirrhosis: a dose-response study. *Dig Dis Sci*. 1996;41:809–815.
7. Schoemaker MH, Gommans WM, Conde de la Rosa L, et al. Resistance of rat hepatocytes against bile acid-induced apoptosis in cholestatic liver injury is due to nuclear factor-kappa B activation. *J Hepatol*. 2003;39:153–161.
8. Keene CD, Rodrigues CM, Eich T, Chhabra MS, Steer CJ, Low WC. Tauroursodeoxycholic acid, a bile acid, is neuroprotective in a transgenic animal model of Huntington's disease. *Proc Natl Acad Sci U S A*. 2002;99:10671–10676.
9. Keene CD, Rodrigues CM, Eich T, et al. A bile acid protects against motor and cognitive deficits and reduces striatal degeneration in the 3-nitropropionic acid model of Huntington's disease. *Exp Neurol*. 2001;171:351–360.
10. Duan WM, Rodrigues CM, Zhao LR, Steer CJ, Low WC. Tauroursodeoxycholic acid improves the survival and function of nigral transplants in a rat model of Parkinson's disease. *Cell Transplant*. 2002;11:195–205.
11. Rodrigues CM, Sola S, Nan Z, et al. Tauroursodeoxycholic acid reduces apoptosis and protects against neurological injury after acute hemorrhagic stroke in rats. *Proc Natl Acad Sci U S A*. 2003;100:6087–6092.
12. Rodrigues CM, Spellman SR, Sola S, et al. Neuroprotection by a bile acid in an acute stroke model in the rat. *J Cereb Blood Flow Metab*. 2002;22:463–471.
13. Castro RE, Amaral JD, Sola S, Kren BT, Steer CJ, Rodrigues CM. Differential regulation of cyclin D1 and cell death by bile acids in primary rat hepatocytes. *Am J Physiol*. 2007;293:G327–G334.
14. Castro RE, Sola S, Ramalho RM, Steer CJ, Rodrigues CM. The bile acid tauroursodeoxycholic acid modulates phosphorylation and translocation of bad via phosphatidylinositol 3-kinase in glutamate-

induced apoptosis of rat cortical neurons. *J Pharmacol Exp Ther*. 2004;311:845–852.

15. Ramalho RM, Borralho PM, Castro RE, Sola S, Steer CJ, Rodrigues CM. Tauroursodeoxycholic acid modulates p53-mediated apoptosis in Alzheimer's disease mutant neuroblastoma cells. *J Neurochem*. 2006;98:1610–1618.
16. Ramalho RM, Ribeiro PS, Sola S, Castro RE, Steer CJ, Rodrigues CM. Inhibition of the E2F-1/p53/Bax pathway by tauroursodeoxycholic acid in amyloid beta-peptide-induced apoptosis of PC12 cells. *J Neurochem*. 2004;90:567–575.
17. Sola S, Castro RE, Kren BT, Steer CJ, Rodrigues CM. Modulation of nuclear steroid receptors by ursodeoxycholic acid inhibits TGF-β1-induced E2F-1/p53-mediated apoptosis of rat hepatocytes. *Biochemistry*. 2004;43:8429–8438.
18. Sola S, Castro RE, Laires PA, Steer CJ, Rodrigues CM. Tauroursodeoxycholic acid prevents amyloid-beta peptide-induced neuronal death via a phosphatidylinositol 3-kinase-dependent signaling pathway. *Mol Med*. 2003;9:226–234.
19. Beuers U, Denk GU, Soroka CJ, et al. Taurolithocholic acid exerts cholestatic effects via phosphatidylinositol 3-kinase-dependent mechanisms in perfused rat livers and rat hepatocyte couplets. *J Biol Chem*. 2003;278:17810–17818.
20. Marzioni M, Francis H, Benedetti A, et al. $Ca2^{+}$-dependent cytoprotective effects of ursodeoxycholic and tauroursodeoxycholic acid on the biliary epithelium in a rat model of cholestasis and loss of bile ducts. *Am J Pathol*. 2006;168:398–409.
21. Dent P, Fang Y, Gupta S, et al. Conjugated bile acids promote ERK1/2 and AKT activation via a pertussis toxin-sensitive mechanism in murine and human hepatocytes. *Hepatology*. 2005;42:1291–1299.
22. Rodrigues CM, Fan G, Wong PY, Kren BT, Steer CJ. Ursodeoxycholic acid may inhibit deoxycholic acid-induced apoptosis by modulating mitochondrial transmembrane potential and reactive oxygen species production. *Mol Med*. 1998;4:165–178.
23. Rodrigues CM, Ma X, Linehan-Stieers C, Fan G, Kren BT, Steer CJ. Ursodeoxycholic acid prevents cytochrome *c* release in apoptosis by inhibiting mitochondrial membrane depolarization and channel formation. *Cell Death Differ*. 1999;6:842–854.
24. Colell A, Coll O, Garcia-Ruiz C, et al. Tauroursodeoxycholic acid protects hepatocytes from ethanol-fed rats against tumor necrosis factor-induced cell death by replenishing mitochondrial glutathione. *Hepatology*. 2001;34:964–971.
25. Boatright JH, Moring AG, McElroy C, et al. Tool from ancient pharmacopoeia prevents vision loss. *Mol Vis*. 2006;12:1706–1714.
26. Chang B, Hawes NL, Pardue MT, et al. Two mouse retinal degenerations caused by missense mutations in the beta-subunit of rod cGMP phosphodiesterase gene. *Vis Res*. 2007;47:624–633.
27. Chang B, Hawes NL, Hurd RE, Davisson MT, Nusinowitz S, Heckenlively JR. Retinal degeneration mutants in the mouse. *Vis Res*. 2002;42:517–525.
28. Bowes C, Li T, Danciger M, Baxter LC, Applebury ML, Farber DB. Retinal degeneration in the rd mouse is caused by a defect in the beta subunit of rod cGMP-phosphodiesterase. *Nature*. 1990;347:677–680.
29. Pittler SJ, Baehr W. Identification of a nonsense mutation in the rod photoreceptor cGMP phosphodiesterase beta-subunit gene of the rd mouse. *Proc Natl Acad Sci U S A*. 1991;88:8322–8326.
30. Gargini C, Terzibasi E, Mazzoni F, Strettoi E. Retinal organization in the retinal degeneration 10 (rd10) mutant mouse: a morphological and ERG study. *J Comp Neurol*. 2007;500:222–238.
31. Grover S, Fishman GA, Anderson RJ, et al. Visual acuity impairment in patients with retinitis pigmentosa at age 45 years or older. *Ophthalmology*. 1999;106:1780–1785.
32. Angulo P, Jorgensen RA, Lindor KD. Incomplete response to ursodeoxycholic acid in primary biliary cirrhosis: is a double dosage worthwhile? *Am J Gastroenterol*. 2001;96:3152–3157.
33. Pardue MT, Phillips MJ, Yin H, et al. Neuroprotective effect of subretinal implants in the RCS rat. *Invest Ophthalmol Vis Sci*. 2005;46:674–682.
34. Pardue MT, Phillips MJ, Yin H, et al. Possible sources of neuroprotection following subretinal silicon chip implantation in RCS rats. *J Neural Eng*. 2005;2:S39–S47.
35. Carter-Dawson LD, LaVail MM. Rods and cones in the mouse retina, I: structural analysis using light and electron microscopy. *J Comp Neurol*. 1979;188:245–262.
36. Daniele LL, Lillo C, Lyubarsky AL, et al. Cone-like morphological, molecular, and electrophysiological features of the photoreceptors of the Nrl knockout mouse. *Invest Ophthalmol Vis Sci*. 2005;46:2156–2167.
37. Bemelmans AP, Kostic C, Crippa SV, et al. Lentiviral gene transfer of RPE65 rescues survival and function of cones in a mouse model of Leber congenital amaurosis. *PLoS Med*. 2006;3:e347.
38. Rohrer B, Lohr HR, Humphries P, Redmond TM, Seeliger MW, Crouch RK. Cone opsin mislocalization in $Rpe65^{-/-}$ mice: a defect that can be corrected by 11-cis retinal. *Invest Ophthalmol Vis Sci*. 2005;46:3876–3882.
39. Hempfling W, Dilger K, Beuers U. Systematic review: ursodeoxycholic acid–adverse effects and drug interactions. *Alimentary Pharmacol Therapeut*. 2003;18:963–972.
40. Wright AF, Jacobson SG, Cideciyan AV, et al. Lifespan and mitochondrial control of neurodegeneration. *Nat Genet*. 2004;36:1153–1158.
41. Berson EL. Long-term visual prognoses in patients with retinitis pigmentosa: the Ludwig von Sallmann lecture. *Exp Eye Res*. 2007;85:7–14.